

The Energy of a Moving Quark-Antiquark Pair in an $\mathcal{N} = 4$ SYM Plasma

Mariano Chernicoff*, J. Antonio García† and Alberto Güijosa‡

Departamento de Física de Altas Energías, Instituto de Ciencias Nucleares

Universidad Nacional Autónoma de México

Apdo. Postal 70-543, México D.F. 04510

Abstract

We make use of the AdS/CFT correspondence to determine the energy of an external quark-antiquark pair that moves through strongly-coupled thermal $\mathcal{N} = 4$ super-Yang-Mills plasma. It is found that the pair feels no drag force, has an energy that reproduces the expected $\sqrt{1 - v^2}/L$ behavior at small quark-antiquark separations, and becomes unbound beyond a certain screening length whose velocity-dependence we determine. We discuss the relation between the high-velocity limit of our results and the lightlike Wilson loop proposed recently as a definition of the jet-quenching parameter.

1 Introduction and Summary

In the past few months, the use of the AdS/CFT correspondence [1, 2, 3] to study energy loss in finite-temperature strongly-coupled gauge theories has attracted significant attention, partly because it is hoped that this line of research could eventually make contact with experimental data from RHIC [4] and ALICE [5].

The drag force experienced by a heavy quark that moves through a thermal $\mathcal{N} = 4$ super-Yang-Mills (SYM) plasma was determined in [6, 7], using its dual description as a string that moves on an AdS-Schwarzschild background. The same information was obtained independently in [8] through a different method, based on an analysis of small string fluctuations (a similar calculation was performed in [6]). Generalizations of the first calculation may be found in [9, 10, 11]. The connection with magnetic confinement was explored in [12]. The directionality of the coherent wake left by the moving quark on the gluonic fields was studied in [13, 14, 15], using the methods of [16, 17].

*e-mail: mariano@nucleares.unam.mx

†e-mail: garcia@nucleares.unam.mx

‡e-mail: alberto@nucleares.unam.mx

An independent approach has aimed at determining the jet-quenching parameter \hat{q} that in phenomenological models of energy loss through medium-induced radiation is meant to codify the average squared transverse momentum transferred to the quark by the medium (for reviews see [18, 19]). Based on the fact that certain approximate calculations in these models relate \hat{q} to a lightlike Wilson loop in the adjoint representation (see [19] and references therein), the authors of [20] suggested that this Wilson loop could be taken to provide a non-perturbative definition of the jet-quenching parameter. Using the simple large- N relation between adjoint and fundamental loops, and the AdS/CFT recipe for the latter¹ [22], they then proceeded to compute this parameter for $\mathcal{N} = 4$ SYM. Their calculation has been generalized in various directions in [23, 24, 11, 27, 28, 29]. Previous related work may be found in [25, 26].

Just like the drag force determination in [6, 7], the calculation of \hat{q} in [20] focuses on a string that moves on an AdS-Schwarzschild background. The difference is that the string considered in [6, 7] has a single endpoint on the boundary, representing the moving external quark, whereas the string studied in [20] has both of its endpoints on the boundary, representing an external quark-antiquark pair that traces out the required lightlike Wilson loop.

In this paper we perform a natural generalization of the above calculations, using the AdS/CFT correspondence to determine the energy of a quark-antiquark pair that moves with velocity v through a strongly-coupled thermal $\mathcal{N} = 4$ SYM plasma. This problem had been previously studied in the case $v = 0$, where the pair is static with respect to the plasma. As expected, the quark-antiquark potential was found to be insensitive to the plasma at small distances, and to display screening behavior beyond a certain length [30, 31]. Analyzing the manner in which these features are modified by the motion of the pair through the plasma is an interesting question in its own right, both from the theoretical and the phenomenological perspectives. Our analysis is additionally motivated by the current discussion on energy loss: the moving quark-antiquark pair serves as a color-neutral probe of the plasma that stands in useful contrast with the solitary quark considered in [6, 7], and moreover, in the $v \rightarrow 1$ limit it would be expected to make contact with the system studied in [20].

Our presentation is organized as follows. In Section 2 we briefly review the salient points of the drag force calculation of [6, 7], and then set up and study the analogous problem for the string on AdS-Schwarzschild that has both of its endpoints on the boundary, satisfying the boundary conditions (11). Below this equation and again after (18) we find that this string feels no drag force, discuss the physical reasons for this result and point out that there exist configurations with the same boundary conditions but different initial conditions where the string *does* experience a drag force. Although framed in the specific context of the background dual to $\mathcal{N} = 4$ SYM, the essence of our arguments is more general and applies to other backgrounds. At the end of Section 2 we derive the basic equations (19)-(23) that determine the shape and energy of the string in the background at hand.

¹An AdS/CFT prescription for directly computing certain Wilson loops in an arbitrary representation of the gauge group was given recently in [21].

Section 3 contains our main results, in SYM language. We open with a discussion on the gauge-theoretic interpretation for the result that the quark-antiquark pair feels no drag force as it ploughs through the $\mathcal{N} = 4$ SYM plasma. After that we carry out the numerical integrations needed to determine the energy of the $q\bar{q}$ pair as a function of the separation L and velocity v . The results are shown in Figs. 3,4. The energy reduces to the expected Coulombic behavior (31) for small separations, and then rises above this behavior due to the effects of the plasma, up to a screening length $L_*(v)$ beyond which the quark and antiquark become unbound. The velocity-dependence of this screening length is shown in Fig. 5; we find it to be well-approximated by (34). For high enough velocities we find a gap in energy between the bound and unbound $q\bar{q}$ configurations, whose physical significance remains unclear to us.

In the closing pages of Section 3 we discuss at length the relation between the $v \rightarrow 1$ limit of our results and the lightlike Wilson loop proposed in [20] as a definition of the jet-quenching parameter \hat{q} . The main lesson is that the AdS/CFT result of [20] cannot be obtained as a smooth limit of standard Wilson loops (11) with $v \rightarrow 1$ from below. We suggest that it should be regarded instead as arising from an approach to $v = 1$ from above. Finally, we note in (36) that, despite the fact that one cannot continuously interpolate between the spacelike worldsheet considered in [20] and the timelike worldsheets studied in the present paper, the $E \propto L^2$ dependence that is central to the definition of the parameter \hat{q} in [20] is in fact available in the $v \rightarrow 1$ limit of a subset of the configurations analyzed here. By analogy with [20], one can then define a parameter K that, at least in this specific example, captures the same information as (and is in close numerical agreement with) \hat{q} .

In the course of our investigation two related papers were posted on the arXiv. While our work was in progress, the paper [32] appeared, whose Section 4.2 discusses drag effects for mesons with spin in a certain confining non-supersymmetric gauge theory, arriving at conclusions which coincide with those of our Section 2. While our paper was in preparation, the work [33] appeared, which analyzes exactly the same quark-antiquark system as we do, focusing on the velocity-dependence of the screening length, which we determine in our Section 3. Their numerical results appear to be in agreement with ours, but as discussed below (34), we find them to be more closely proportional to $(1 - v^2)^{1/3}$ than to the $(1 - v^2)^{1/4}$ reported in [33].

2 Nambu-Goto String in AdS-Schwarzschild

As mentioned in the Introduction, the computation in [6, 7] of the drag force felt by an external quark moving through $\mathcal{N} = 4$ SYM plasma focuses on a string that extends all the way from the boundary to the horizon of an AdS-Schwarzschild geometry, i.e., from $r \rightarrow \infty$ to $r = r_H$, with r an appropriate radial coordinate that we will henceforth also use as spatial worldsheet coordinate. We will in addition employ the boundary time $t = x^0$ as worldsheet time, so altogether we work in the static gauge

$$\sigma = r, \quad \tau = t . \tag{1}$$

The dynamics of the string are described by the Nambu-Goto action

$$S = -\frac{1}{2\pi\alpha'} \int d\tau d\sigma \sqrt{-\det g_{\alpha\beta}} \equiv -\frac{1}{2\pi\alpha'} \int d\tau d\sigma \mathcal{L} , \quad (2)$$

where $G_{\mu\nu}$ is the spacetime metric and $g_{\alpha\beta} \equiv G_{\mu\nu} \partial_\alpha X^\mu \partial_\beta X^\nu$ the induced worldsheet metric. The force that a given segment of the string exerts along spatial direction i on the neighboring segment was expressed in [7] as

$$F_i = -\frac{1}{2\pi\alpha'} \sqrt{-g} P_i^r , \quad (3)$$

with

$$P_\mu^\alpha = g^{\alpha\beta} \partial_\beta X_\mu \quad (4)$$

the worldsheet current associated with spacetime momentum, whereas in [6] it was formulated as

$$F_i = -\frac{1}{2\pi\alpha'} \Pi_i^r , \quad (5)$$

with

$$\Pi_\mu^\alpha = \frac{\partial \mathcal{L}}{\partial(\partial_\alpha X^\mu)} \quad (6)$$

the canonical momentum densities conjugate to X^μ . By explicitly inverting the 2×2 matrix $g_{\alpha\beta}$, one can easily verify that

$$\sqrt{-g} P_\mu^\alpha = \Pi_\mu^\alpha , \quad (7)$$

and so the expressions (3) and (5) coincide. Clearly the latter is simpler to use in explicit computations.

The crucial point in the calculation of [6, 7] is the observation that, if this string is assumed to travel at constant velocity $v \neq 0$ along a direction $x = x^1$ parallel to the boundary, then there is a certain velocity-dependent value of the radial coordinate,

$$r_v = \frac{r_H}{(1 - v^2)^{1/4}} , \quad (8)$$

below which the embedding function

$$X(r, t) = vt + \xi(r) \quad (9)$$

for the string would become imaginary. The only way to avoid this is to let the string trail behind its boundary endpoint following a specific profile $\xi(r) \neq \text{constant}$, which translates into a specific value for the drag force F_x exerted on the endpoint. In short, the non-zero value of the drag force is set uniquely by the condition that the string crosses the critical radius r_v .

In this section we are interested in exploring how these considerations generalize to a moving string that has *both* of its endpoints on the boundary, and is therefore dual not to a single quark but to a quark-antiquark pair in the gauge theory.

Since the string now extends first away from and then back to the boundary, the static gauge choice $\sigma = r$ leads of course to a double-valued parametrization, but this poses no problem other than the need to check by hand that the two halves of the string join together smoothly (which ensures that the action is extremized not just piecewise, but over the entire worldsheet). To describe a moving quark-antiquark pair, both of the string endpoints are taken to travel with the same velocity v in the x direction, and to be separated by a constant distance L along a certain boundary direction $y = x^2$. In other words, with a convenient choice of origin, the embedding functions (9) and

$$Y(r, t) = Y(r) \tag{10}$$

satisfy the boundary conditions

$$X(\infty, t) = vt, \quad Y(\infty) = \mp \frac{L}{2}, \tag{11}$$

where the upper (lower) signs refer to the left (right) half of the string. For concreteness, we specialize immediately to the case where y is perpendicular to the direction of motion x , which among other reasons is of particular interest in view of the connection with [20]. The string starts at $r \rightarrow \infty$ and extends down to a minimal radius r_{min} , which by symmetry is such that $Y(r_{min}) = 0$ and $Y'(r_{min}) = \infty$ (which is of course the condition that the projections of the two halves of the string onto the $r - y$ plane can be glued together smoothly).

The main question is whether such a string also trails behind its endpoints and exerts a drag force on them, as would seem compulsory if the string crosses r_v , and might appear natural more generally on physical grounds. The shape of the string would then be similar to that shown in Fig. 1a. It is easy to see, however, that this cannot happen. The reason is that, on the one hand, the force along the direction of motion must vanish at the midpoint ($r = r_{min}$), because by symmetry the string at that point must be perpendicular to the x -axis, and on the other hand, the force must be constant along the string, because each of its segments moves at constant velocity. We conclude then that $F_x = 0$ everywhere, which implies that the string remains upright, as in Fig. 1b.

Since we initially envisioned the string as being pulled along from its endpoints, it might seem somewhat counterintuitive that it does not lean backward. To clarify this point, it is worth noting that the r -independence of $F_x = \Pi_x^r$ is a consequence of the equation of motion for X (or, equivalently, the covariant conservation law for the momentum current P_x^α),

$$\partial_t(\Pi_x^t) + \partial_r(\Pi_x^r) = 0, \tag{12}$$

where the first term vanishes due to the trivial time-dependence of the embedding functions (9) and (10) (while the right-hand side vanishes because \mathcal{L} is independent of X). From this it becomes clear that the conclusion of the previous paragraph can be avoided, and the string can lean backward, if and only if it displays a more complicated time dependence (e.g., some type of oscillatory behavior).

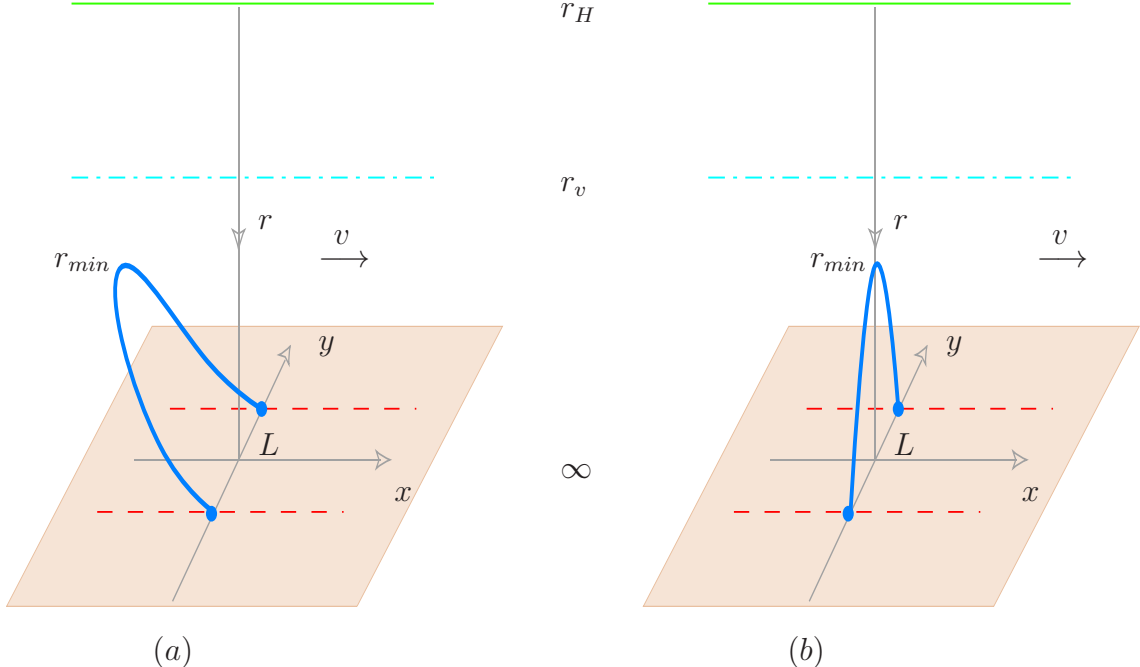


Figure 1: Sketch of the string dual to a moving quark-antiquark pair. The radial coordinate runs downward, so the horizon at $r = r_H$ is shown at the top and the boundary at $r \rightarrow \infty$ is represented by the plane at the bottom. The dash-dot line at $r = r_v$ marks a velocity-dependent radius beyond which the string cannot penetrate. As the string moves to the right, its endpoints (dual to the external quark and antiquark) trace out the dotted trajectories. Its shape codifies information on the configuration of the SYM color fields. (a) One might expect the string to lean backward as a result of the motion. This turns out to be possible only if the string has a nontrivial time-dependence. (b) The lowest-energy configuration for the moving string is in fact upright, similar to the one obtained in the static case. See text for further discussion.

The basic issue here is a familiar one: specifying boundary conditions for the string does not select a unique solution to the corresponding equation of motion; one must additionally specify initial conditions. If the string is initially upright and moving as a whole at velocity v , then as we have seen it will continue to do so, and its endpoints will trace the required paths without requiring an external agent that pulls on them in the direction of motion. On the other hand, if the string is initially static and *then* we start pulling its endpoints with whatever force is necessary for them to move at constant velocity v , the string *will* of course lean backward, as in Fig. 1a. What we have learned above, however, is that such a string will continue to oscillate and will never (classically) stabilize to a configuration of the type (9). The solution in question is therefore clearly not the one with the lowest energy for the given boundary conditions. Nevertheless, as we will see in the next section, there are circumstances under which this type of solution might conceivably play a role in the computation of the energy for the quark-antiquark system of interest to us.

We should similarly keep in mind that it is possible to satisfy the boundary conditions (11) with two *separate* strings that reach all the way down from the boundary to the horizon at fixed $Y = \mp L/2$, trailing behind their endpoints as described in [6, 7]. Such configuration would clearly describe an unbound quark and antiquark, and it will also be of relevance below.

Let us now proceed towards the determination of the shape of the moving string in the AdS-Schwarzschild background. Using the explicit form of the metric²

$$ds^2 = \frac{1}{\sqrt{H}} \left(-h dt^2 + d\vec{x}^2 \right) + \frac{\sqrt{H}}{h} dr^2, \quad (13)$$

$$H = \frac{R^4}{r^4}, \quad h = 1 - \frac{r_H^4}{r^4},$$

together with the embedding functions (9) and (10), the Lagrangian (2) simplifies to

$$\mathcal{L} = \sqrt{-g} = \sqrt{1 + \frac{h}{H} (X'^2 + Y'^2) - \frac{v^2}{H} Y'^2 - \frac{v^2}{h}}. \quad (14)$$

As already noted above, given that the string moves at constant velocity and \mathcal{L} is independent of X , the corresponding equation of motion (12) is just the statement that the conjugate momentum density Π_x^r is a (real) constant, which we will denote Π_x in what follows. The same is of course true for $\Pi_y \equiv \Pi_y^r$. According to (5), these constants determine the forces F_x and F_y that an external agent must exert on the string endpoints to satisfy the given Dirichlet boundary conditions (11).

Inverting the definitions (6) to express X' and Y' in terms of the constants Π_x and Π_y we obtain

$$X' = \Pi_x \frac{(h - v^2)}{h} \sqrt{\frac{H}{(h - v^2)(\frac{h}{H} - \Pi_x^2) - h\Pi_y^2}}, \quad (15)$$

$$Y' = \mp \Pi_y \sqrt{\frac{H}{(h - v^2)(\frac{h}{H} - \Pi_x^2) - h\Pi_y^2}}, \quad (16)$$

where we notice the appearance of the same factor $h - v^2$ whose vanishing defined the critical radius (8) that as explained above played a crucial role in fixing the value

$$\Pi_x = \frac{v}{\sqrt{1 - v^2}} \quad (17)$$

for the string dual to a moving quark [6, 7].

There are two immediate things we can learn from the above equations. First, we see from (16) that Y' diverges at the point where the denominator vanishes; according to the characterization following (10) this defines the turnaround point r_{min} :

$$\left[(h - v^2) \left(\frac{1}{H} - \frac{\Pi_x^2}{h} \right) \right]_{r=r_{min}} = \Pi_y^2. \quad (18)$$

²The relevant background is as usual (AdS-Schwarzschild)₅ × **S**⁵, but we display only the metric for the first factor because the string is taken to lie at a fixed position on the **S**⁵.

It is easy to show from this expression that $r_{min} \geq r_v$, where equality holds only if $\Pi_y = 0$ (which would imply $L = 0$). So, as expected, we find that the string dual to the moving quark-antiquark pair cannot penetrate beyond the critical radius r_v .

Second, in order for the projections of the two halves of the string onto the $y - x$ plane to join smoothly, we must require that $\partial Y/\partial X = Y'/X' = \infty$ at r_{min} , but taking the quotient of (16) and (15) we see that this is *not* possible unless $\Pi_x = 0$, and therefore $X' = 0$. So, as we had already anticipated, we learn that the string can only move at constant speed if it is upright. This same conclusion has been reached independently in [32].

Specializing (16), (18) and (14) to the case $X' = 0$ ($\Rightarrow \xi(r) = 0$), we can now summarize the equations that will be of interest to us in the remainder of this paper. The profile of the upright string that moves with velocity v and has endpoint separation L is determined by

$$Y' = \mp \Pi_y \frac{R^4}{\sqrt{(r^4 - r_H^4)(r^4(1 - v^2) - r_H^4 - R^4 \Pi_y^2)}} , \quad (19)$$

where the value of Π_y must be chosen in such a way that

$$L = 2 \int_{r_{min}}^{\infty} dr Y' = 2 \Pi_y R^4 \int_{r_{min}}^{\infty} \frac{dr}{\sqrt{(r^4 - r_H^4)(r^4(1 - v^2) - r_H^4 - R^4 \Pi_y^2)}} , \quad (20)$$

with

$$r_{min} = \left(\frac{r_H^4 + R^4 \Pi_y^2}{1 - v^2} \right)^{1/4} . \quad (21)$$

Using (19), the Lagrangian density (14) reduces to

$$\mathcal{L} = \frac{r^4(1 - v^2) - r_H^4}{\sqrt{(r^4 - r_H^4)(r^4(1 - v^2) - r_H^4 - R^4 \Pi_y^2)}} . \quad (22)$$

Close to the boundary we find $\mathcal{L} \rightarrow \sqrt{1 - v^2}$, which upon integration implies that the total worldsheet area per unit boundary time is linearly divergent. But as usual, the same divergence is found in the area of the two disconnected worldsheets dual to the unbound quark and antiquark, described by (14)-(16) with $\Pi_y = 0$ and Π_x as in (17), which results in $\mathcal{L}_{unbound} = \sqrt{1 - v^2}$. Subtracting the two areas we find a finite expression³ for the energy of the quark-antiquark pair relative to that of the unbound system,

$$E = \frac{2}{2\pi\alpha'\mathcal{T}} \int_{-\mathcal{T}/2}^{+\mathcal{T}/2} dt \left(\int_{r_{min}}^{\infty} dr \mathcal{L} - \int_{r_H}^{\infty} dr \mathcal{L}_{unbound} \right) . \quad (23)$$

³In more accurate language, one should as usual introduce a regulating surface at a large radius $r = r_\Lambda$ to make both integrals finite, subtract and in the end take $r_\Lambda \rightarrow \infty$. In the dual gauge theory, this is equivalent to introducing a UV cutoff $\Lambda \simeq r_\Lambda/R^2$.

3 Energy of Moving Quark-Antiquark System

In this section we will use the above results for the moving string to make various inferences about the dual system: an external quark-antiquark pair in $SU(N)$ $\mathcal{N} = 4$ SYM with 't Hooft coupling $g_{YM}^2 N$ and temperature T determined by the AdS radius R , horizon radius r_H and string length $\sqrt{\alpha'}$ through [3]

$$g_{YM}^2 N = \frac{R^4}{\alpha'^2}, \quad T = \frac{r_H}{\pi R^2}. \quad (24)$$

According to (5), the fact that $\Pi_x = 0$ translates into the statement that, in stark contrast with the solitary quark considered in [6, 7], an external quark-antiquark pair feels no drag force as it ploughs through the plasma, a curious result that was obtained independently in the recent paper [32].

As explained in [6, 7] and analyzed more closely in [13, 14, 15], a moving quark produces an extended wake in the color fields, which may be regarded as a coherent spray of gluons radiated away from the quark, and is the CFT dual of the trailing string that extends all the way down to the horizon. It is this wake that transports energy and momentum away from the quark and into the surrounding medium. It is worth noting that this mechanism can operate even at zero temperature, where there is no plasma: given appropriate initial conditions for the gluonic fields, a quark moving at constant speed *can* lose energy to the wake it imprints on these fields. The dual statement is that a string on pure AdS that displays a non-trivial time-dependence *can* trail behind its boundary endpoint even if the latter moves at constant velocity.⁴ This, of course, should not come as a surprise, because the SYM vacuum constitutes, after all, a highly nonlinear polarizable medium. Needless to say, the lowest-energy configuration for the gluonic field profile surrounding the moving quark at zero temperature is the one obtained by boosting the static profile; this configuration is dual to an upright string, which feels no drag force. The string considered in [6, 7] correctly reduces to this case when $T \rightarrow 0$, which ensures that the energy loss process studied there is intrinsically associated with the presence of the plasma.

Unlike the single quark, which carries a net color charge, the quark-antiquark pair is a dipole, and consequently sets up a shorter-ranged profile in the gluonic fields. At zero-temperature, the dipolar $\text{Tr } F^2$ falloff is proportional to L^3/r^7 [17, 34], compared to the Coulomb-like $1/r^4$ of the monopole [16]. At finite temperature, we have learned here that the profile generated by the moving pair is not able to transport energy away from it, a property that could plausibly be verified using the methods of [13, 14, 15]. In the $N \gg 1$, $g_{YM}^2 N \gg 1$ regime of the gauge theory that is captured by classical string theory on weakly-curved AdS-Schwarzschild, no other mechanism of energy loss is at work, and so the quark-antiquark pair moves through the plasma unimpeded. This result should generalize to any color-neutral probe of the plasma, including the baryon, whose static AdS dual was constructed in [35, 36, 37] and whose

⁴The assertion for the string may be deduced from an argument similar to the discussion following (12); its SYM dual could be verified through calculations similar to those performed in [17].

zero-temperature $\text{Tr } F^2$ falloff is also $\propto r^{-7}$ [17]. The remarks we made above for the solitary quark at $T = 0$ apply as well to these color-neutral systems at $T > 0$: with a different set of initial conditions for the gluonic fields, the quark-antiquark pair and the baryon *can* experience a drag force.

Let us now proceed to determine the energy E of the moving quark-antiquark pair for a given velocity v and separation L . For this we first need to carry out the integrals (20) and (23) to find $L(\Pi_y, v)$ and $E(\Pi_y, v)$, and then eliminate Π_y to obtain $E(L, v)$. As indicated in (3) and explained in the discussion below (14), Π_y is a measure of the force F_y that an external agent must exert in order to keep the $q\bar{q}$ pair at the desired separation.

Unfortunately, the integrals cannot be performed analytically, so we must solve the problem numerically. For this purpose, it is convenient to use $h = 1 - r_H^4/r^4$ in place of r as the integration variable. The range of integration should then be taken from

$$h_{min} \equiv h(r_{min}) = \frac{2 - v^2 + f_y^2}{1 + f_y^2} \quad (25)$$

to 1, where we have defined the rescaled force

$$f_y \equiv \frac{R^2}{r_H^2} \Pi_y = \frac{2}{\pi \sqrt{g_{YM}^2 N T^2}} F_y .$$

The result $r_{min} > r_v$ of the previous section translates into $h_{min} > v^2$, which can also be easily deduced from (25). After changing variables in this manner and using the dictionary (24), the expressions for the quark-antiquark separation (20) and energy (23) turn into

$$L(f_y, v) = \frac{f_y}{2\pi T} \int_{h_{min}}^1 \frac{dh}{(1-h)^{\frac{1}{4}} \sqrt{(h-v^2)h - (1-h)hf_y^2}} , \quad (26)$$

and

$$E(\pi_y, v) = \frac{T \sqrt{g_{YM}^2 N}}{4} \left[\int_{h_{min}}^1 \frac{dh(h-v^2)}{(1-h)^{\frac{5}{4}} \sqrt{(h-v^2)h - (1-h)hf_y^2}} - \int_0^1 \frac{\sqrt{1-v^2} dh}{(1-h)^{\frac{5}{4}}} \right] . \quad (27)$$

As noted at the end of the previous section, the subtraction implemented by the second term in equation (27) ensures a finite result and corresponds to removing the self-energies of the quark and antiquark moving separately through the plasma.

The results of the numerical integration of (26) are shown in Fig. 2, which displays

$$l \equiv 2\pi T L$$

as a function of the applied external force f_y for a few different values of v . The behavior is in all cases qualitatively the same as was found in [30, 31] for the static case: at any given v , it is only possible to attain separations in a finite range $0 \leq L \leq$

$L_{max}(v)$, and each separation in this range can be achieved with two different values of the force F_y . The exception is of course the maximum $L_{max}(v)$, whose physical meaning will become clear below, and which we find empirically to be located at a value of the external force that varies roughly in a linear manner with the velocity,

$$f_{y_{max}}(v) \simeq 0.8 + 0.6v .$$

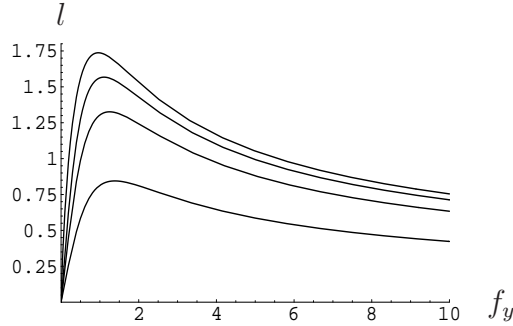


Figure 2: Quark-antiquark separation (in units of $1/2\pi T$) as a function of the applied external force (in units of $\pi\sqrt{g_{YM}^2 NT^2/2}$), for velocities $v = 0, 0.45, 0.7, 0.95$. Lower curves correspond to larger velocities.

Combining these results with the numerical integration of (27), we can find the quark-antiquark energy $E(L, v)$ for any velocity $0 \leq v \leq 1$ and separation $0 \leq L \leq L_{max}(v)$. The results are plotted in Figs. 3 and 4, which display

$$e \equiv \frac{4}{\sqrt{g_{YM}^2 NT}} E$$

as a function of l , for a few representative values of v . In each case the curve is divided into two parts: a dashed portion obtained from the smaller value of the applied force consistent with the given separation L (i.e., $f_y < f_{y_{max}}$), and a solid portion obtained from the larger value ($f_y \geq f_{y_{max}}$). As we can see in the figures, it is this latter case that gives the lower value for the quark-antiquark energy, and consequently the solid curve describes the stable configurations that are of most interest to us. The dashed curve is associated instead with configurations that are physical and can be selected through a proper choice of initial conditions for the gluonic fields in SYM (or, in dual language, for the string in AdS-Schwarzschild), but are only metastable (i.e., they are stable under small, but not arbitrary, fluctuations).

In Fig. 3a we verify that for the static configuration $v = 0$ we correctly reproduce the $q\bar{q}$ potential computed in [30, 31], which, as explained there, encodes all of the expected physics. At small separations (large energies) the quark-antiquark pair becomes insensitive to the plasma and as a result the potential approaches the $1/L$ behavior obtained at $T = 0$ in [22]. As the separation grows, however, the effects of the plasma progressively screen the quark and antiquark from one another,

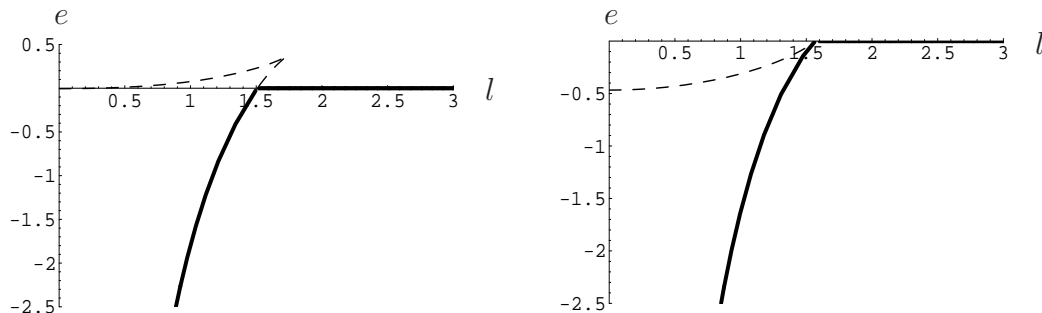


Figure 3: Quark-antiquark energy (in units of $T\sqrt{g_{YM}^2 N}/4$) as a function of separation (in units of $1/2\pi T$), for (a) $v = 0$ (b) $v = 0.45$. The solid (dashed) portion of each curve corresponds to stable (metastable) configurations.

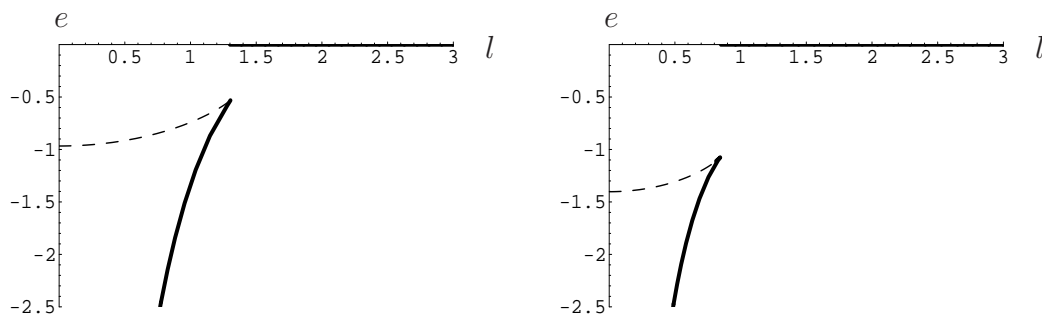


Figure 4: Quark-antiquark energy (in units of $T\sqrt{g_{YM}^2 N}/4$) as a function of separation (in units of $1/2\pi T$), for (a) $v = 0.7$, (b) $v = 0.95$. The solid (dashed) portion of each curve corresponds to stable (metastable) configurations.

and as a consequence raise the system's energy above the Coulombic behavior. The screening becomes complete at the distance $L_* \approx 1.5/2\pi T < L_{max}(0)$ where the energy matches that of the unbound system. For separations larger than this screening length, the quark and antiquark are free and the $q\bar{q}$ potential vanishes, as indicated by the horizontal solid line. The configurations described by (26) and (27) in the range $L_* < L \leq L_{max}$ are only metastable, which is why the corresponding portion of the curve is also dashed.

As seen in Figs. 3 and 4, the results for $v > 0$ have many similarities with the static case. The main overall effect of increasing the velocity is to move the $E(L)$ curve to the left and down, but the latter behavior is not quite monotonic. The dependence of L_{max} on the velocity is given by the solid line in Fig. 5. We find it to be quite close to

$$L_{max}(v) \simeq \frac{1.73}{2\pi T} (1 - v^2)^{1/3}, \quad (28)$$

shown as the long-dash line in the figure.

The energy at this maximum separation, $E_{max}(v) \equiv E(L_{max}, v)$ is shown as a function of velocity in Fig. 6. For small velocities this energy decreases, passing through zero at a velocity ~ 0.447 . E_{max} then reaches a minimum value ~ -1.07

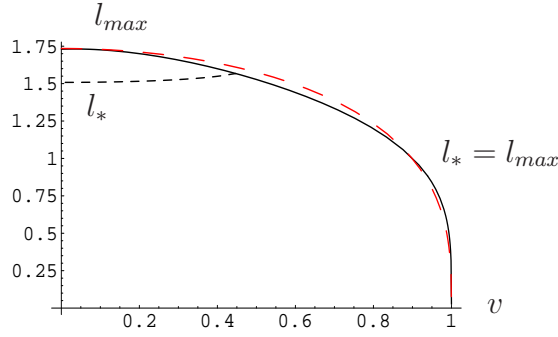


Figure 5: Maximum quark-antiquark distance L_{max} and screening length L_* as functions of the velocity. Both lengths are given in units of $1/2\pi T$.

at velocity ~ 0.97 , after which it quickly returns to zero. We find that the graph is practically indistinguishable from that of the function

$$E_{max}(v) \simeq \frac{0.368T\sqrt{g_{YM}^2 N}}{4}(1-5v^2)(1-v^2)^{1/12}.$$

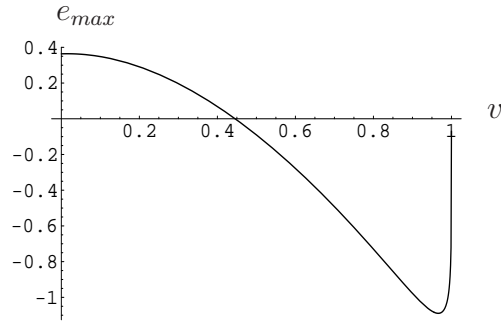


Figure 6: Maximum energy as a function of v , in units of $T\sqrt{g_{YM}^2 N}/4$.

For any velocity, we expect the presence of the plasma to become irrelevant at short distances, so at small L our results should approach the corresponding zero-temperature curves. The latter can be determined analytically. By taking the $T \rightarrow 0$ limit in (26), (27) and (21) we obtain

$$L = 2R^4\Pi_y \int_{r_{min}}^{\infty} \frac{dr}{r^2\sqrt{(1-v^2)r^4 - R^4\Pi_y^2}} \quad (29)$$

and

$$E = \frac{1}{\pi\alpha'} \left[\int_{r_{min}}^{\infty} \frac{r^2(1-v^2)dr}{\sqrt{(1-v^2)r^4 - R^4\Pi_y^2}} - \int_0^{\infty} \sqrt{1-v^2}dr \right], \quad (30)$$

with $r_{min} = R\sqrt{\Pi_y}/(1-v^2)^{1/4}$. Changing to the dimensionless integration variable $\rho \equiv (1-v^2)^{1/4}r/R\sqrt{\Pi_y}$, it is possible to find an explicit relation between E and L ,

$$E(L, v) = -\frac{4\pi^2\sqrt{g_{YM}^2 N}\sqrt{1-v^2}}{\Gamma(\frac{1}{4})^4 L}. \quad (31)$$

For $v = 0$ we recover the static result obtained some years ago in [22]. The $\sqrt{1-v^2}$ dependence is as dictated by Lorentz invariance.⁵ We have checked that our results for $E(L, v)$ at finite temperature correctly approach (31) at small separation. The reason for this agreement is evident from the string theory side: the limit $L \rightarrow 0$ implies that $r_{min} \rightarrow \infty$, so for small separations the string does not penetrate far into the AdS-Schwarzschild geometry, and it is difficult for it to sense the difference with pure AdS.

The behavior of the full $E(L, v)$ graph for small velocities is essentially the same as in the static case. As the velocity increases, the screening length $L_*(v)$ (which we always define as the separation beyond which the quark and antiquark become unbound) is found to increase slowly, as shown by the short-dash line in Fig. 5. The dependence is nearly quadratic,

$$L_*(v) \simeq \frac{1.5}{2\pi T} \left(1 + \frac{1}{3}v^2\right) \quad \text{for small } v. \quad (32)$$

As seen in the same figure, $L_{max}(v)$ is monotonically decreasing, so there is a velocity $v_{gap} \sim 0.447$ at which both lengths coincide; this is precisely the first zero in Fig. 6.

For $v > v_{gap}$, both types of bound solutions (stable and metastable) have negative energy, so a gap begins to develop between the bound and unbound configurations, whose width evolves as indicated in the negative portion of the graph in Fig. 6. The maximum width of the gap is quite large, of order $\sqrt{g_{YM}^2 NT}$. It is therefore natural to wonder whether at $v > v_{gap}$ there could be additional *bound* $q\bar{q}$ configurations which cover a range of separations $L > L_{max}$, and consequently narrow or perhaps even eliminate the gap. As discussed earlier in this section, there certainly exist configurations in which the quark and antiquark move at constant velocity but the color fields display a more complicated time dependence. Their AdS description was discussed in the paragraphs that follow (12); it involves a string that leans back as in Fig. 1a and has time dependence beyond the overall motion at velocity v . These configurations exist both for $L \leq L_{max}$ and $L > L_{max}$, but in the former case they are clearly metastable and therefore not of interest for the present discussion. What is not at all obvious to us is whether at least one of the configurations for $L > L_{max}$ manages to have negative energy. This is a complicated question that would appear to require numerical exploration of the space of solutions to the corresponding coupled partial differential equations.

⁵This dependence was also noted recently in [12], which includes some comments on the finite-temperature behavior of $E(L, v)$ in the ladder approximation of the gauge theory.

In the remainder of this paper we assume that for all values of L and v , the lowest energy configurations are always the ones with the simplest time dependence: for $L < L_{max}$, the bound $q\bar{q}$ system dual to the upright string in Fig. 1b; for $L > L_{max}$, the unbound quark and antiquark dual to two separate copies of the string analyzed in [6, 7]. The graphs in Figs. 3,4 can then be taken at face value, and imply in particular that for $v > v_{gap}$ the screening length should be identified with the location of the discontinuity in $E(L)$, i.e., $L_*(v) = L_{max}(v)$, or according to (28),

$$L_*(v) \simeq \frac{1.73}{2\pi T} (1 - v^2)^{1/3} \quad \text{for } v > 0.447. \quad (33)$$

Combining this with (32), we obtain the simple expression

$$L_*(v) \simeq \frac{1.5}{2\pi T} \left(1 + \frac{1}{3}v^2\right) (1 - v^2)^{1/3} \quad \text{for } 0 \leq v \leq 1. \quad (34)$$

As seen in these last two equations, for large velocities the screening length $L_*(v)$ decreases monotonically to zero, implying that $E(L, v) = 0$ everywhere except in the rapidly shrinking range $0 < L < L_*(v)$, where the behavior (for the stable configurations) is close to the Coulombic (31).

The AdS/CFT prediction for the velocity-dependence of the screening length was the main subject of [33], which appeared while this paper was in preparation. The authors of that work did not compute $E(L, v)$, and consequently defined the screening length not as L_* but as the maximum allowed separation L_{max} , throughout the entire range of velocities. Their equations and numerical results appear to be in agreement with ours, but we find that the $L_{max}(v)$ curve is closer to (28) than to the $(1 - v^2)^{1/4}$ they report.

In the $v \rightarrow 1$ limit the Wilson loop traced by our moving quark-antiquark pair approaches the lightlike loop used in [20] to propose a non-perturbative definition of the jet-quenching parameter \hat{q} .⁶ We would have therefore expected our results to make contact with those of [20] in this limit, and were surprised to find that this is not the case. The difference is drastic: whereas the string of [20] extends all the way from the boundary to the horizon and back, in the $v \rightarrow 1$ limit the string that we use to describe bound configurations explores only an ever-shrinking region of the geometry close to the boundary.⁷

The main obstruction to a continuous interpolation between our results and those of [20] is the fact that for any value of v we have found and employed string worldsheets whose area is real, whereas the authors of [20] work with a worldsheet whose area is imaginary. The difference does not appear to be attributable to the fact that their Wilson loop is strictly lightlike, while ours is (in general) only approximately

⁶To be more precise, one should take $v \rightarrow -1$ to agree with the conventions of [20].

⁷One should of course remember that such strings are allowed only for separations smaller than the screening length, which approaches zero in the high-velocity limit. For larger separations the system is unbound, and involves two separate strings which do extend from the boundary to the horizon, but are still quite distinct from the string considered in [20].

so, because the gauge theory calculations which motivate the connection to the jet-quenching parameter build upon an eikonal approximation justified in terms of a high energy limit which manifestly takes $v \rightarrow 1$ from below [19, 39]. Moreover, an argument has recently been given in [33, 38] to the effect that the result for the lightlike Wilson loop of [20] can be obtained continuously from Wilson loops that correspond to velocities that approach $v = 1$ from below. The key point is that, for any given $v < 1$, the authors of [20, 33] enforce boundary conditions for the string not at the AdS-Schwarzschild boundary, but at a finite radius $r = r_{LRW} \ll r_v$ (with r_v the critical radius given in (8)). As a result of this, their worldsheet lies entirely in the region $r < r_v$, which is inaccessible to a string that reaches the boundary, as do the strings considered in the present paper. This explains why the worldsheets that lead to the result of [20] are spacelike.

Regrettably, we do not understand the physics behind this prescription. One can envision of course situations where the choice of boundary conditions for a path integral result in its being dominated by a saddle point with imaginary action,⁸ but we do not see why this should be the case in the problem at hand. To determine the value of a Wilson loop traced by a $q\bar{q}$ pair that moves at any velocity smaller than, but *arbitrarily close* to, the speed of light, the AdS/CFT recipe [22] requires the string boundary conditions (11) to be enforced at $r \rightarrow \infty$, because it is only in this limit that the dual quark and antiquark become pointlike. Since this limit is taken at fixed v , the string in question will have no choice but to lie entirely in the $r > r_v$ region, so its worldsheet will be timelike, and the predicted value for the Wilson loop at strong coupling will unambiguously coincide with the result $\exp[iE(L, v)]$ obtained in this paper.

If the string boundary conditions (11) are enforced instead as advocated in [20, 33, 38], the string endpoints lie at a finite radius $r = r_{LRW} \ll r_v$. In this case the path integral for the string is indeed dominated by a saddle point with imaginary action, a condition which has been argued [33, 38, 39] to be necessary in order to make contact with the jet-quenching parameter defined in phenomenological models of energy loss. But by the standard UV/IR reasoning [40], this path integral would appear to be computing not a standard but a ‘thick’ Wilson loop, traced by sources for the gluonic field that have a characteristic size $d \sim R^2/r_{LRW} \gg R^2/r_v \simeq (1 - v^2)^{1/4}/T$ (which according to (33) happens to be much larger than the screening length at the given v). It is unclear to us whether this thick loop is in some way relevant to the approximate gauge theory calculations [19] that motivated the proposal of [20]. One should not of course lose sight of the fact that the loop becomes ‘thinner’ (in the sense that $d \rightarrow 0$) as $v \rightarrow 1$, so precisely at $v = 1$ one is computing a standard Wilson loop (with a string worldsheet that correctly extends all the way to the AdS-Schwarzschild boundary). But, as already noted above, the gauge theory basis for the definition of [20] would appear to allow a smooth approach via *standard* Wilson loops with $v \rightarrow 1$ from below, which the AdS/CFT correspondence would compute using timelike worldsheets up to

⁸A simple example is provided by the computation of the propagator for a free relativistic particle moving across a spacelike interval.

and including $v = 1$ (where we would find $E(L, v = 1) = 0$). Perhaps a more useful characterization of the $v = 1$ Wilson loop computed in [20] is as a smooth limit of standard Wilson loops with $v \rightarrow 1$ from *above*.

Before leaving this subject, it is interesting to note that the $E \propto L^2$ dependence that was called for in the definition of \hat{q} proposed in [20]— a dependence that was successfully obtained in that work using the spacelike worldsheets discussed in the preceding paragraphs— can also be coaxed out of the $v \rightarrow 1$ limit of the *time-like* worldsheets analyzed in this paper, by focusing not on the stable but on the metastable (dashed) portions of the $E(L, v)$ curves of Fig. 4 that lie near the intersection with the E axis. This region corresponds to configurations with small separations and small applied external forces, $f_y \ll 1$. Using this condition it is straightforward to infer from (26) and (27) and that, at next-to-leading order in L ,

$$E(L) = \frac{T(g_{YM}^2 N)^{\frac{1}{2}}}{4} \left[\int_{h_{min}}^1 \frac{\sqrt{h-v^2} dh}{\sqrt{h}(1-h)^{\frac{5}{4}}} - \int_0^1 \frac{\sqrt{1-v^2} dh}{(1-h)^{\frac{5}{4}}} \right] + \frac{L^2 T^3 \pi^2 (g_{YM}^2 N)^{\frac{1}{2}}}{2} \left[\int_{h_{min}}^1 \frac{dh}{(1-h)^{\frac{1}{4}} \sqrt{h(h-v^2)}} \right]^{-1}, \quad (35)$$

i.e., the energy depends quadratically on the q - \bar{q} separation, as desired. In the limit $v \rightarrow 1$, this relation implies

$$E(L) = \frac{\sqrt{2}}{4} (1-v^2)^{1/4} [A + KL^2], \quad (36)$$

$$A = \frac{\sqrt{\pi} \Gamma(-\frac{1}{4})}{2\sqrt{2} \Gamma(\frac{5}{4})} \sqrt{g_{YM}^2 NT}, \quad K = \frac{\pi^{3/2} \Gamma(\frac{1}{4})}{2\sqrt{2} \Gamma(\frac{3}{4})} \sqrt{g_{YM}^2 NT^3},$$

where the numerical prefactor in the first equation has been chosen according to the normalization used in [20], in order to make K directly comparable to \hat{q} . Independently of whether or not there exists some argument relating the coefficient K to the jet-quenching parameter as defined in phenomenological models [18, 19], this calculation shows that the information encoded in the parameter \hat{q} defined in [20] can also be accessed using the timelike worldsheets studied in the present paper. This is especially interesting in view of the fact that in the $v \rightarrow 1$ limit, such worldsheets never wander far from the AdS-Schwarzschild boundary. Due to the conformal invariance of the underlying gauge theory, the temperature-dependence of the parameters K and \hat{q} was bound to agree. The agreement in their 't Hooft-coupling dependence is also not particularly surprising. What is perhaps worth noting is that the numerical coefficients are practically equal,

$$K = (\Gamma(1/4)^4 / 16\pi^2) \hat{q} \approx 1.1 \hat{q}.$$

In the absence of a direct gauge (or string) theory link between these two parameters, it might be worth exploring their relation in other gauge theories with known gravity duals.

Acknowledgements

It is a pleasure to thank Elena Cáceres for collaboration in the initial stages of this work, for valuable discussions, and for useful comments on the manuscript. We are also grateful to Chris Herzog, Krishna Rajagopal and Urs Wiedemann for helpful correspondence, and to David Vergara for pointing out a number of relevant references. This work was partially supported by Mexico's National Council of Science and Technology (CONACyT) grants CONACyT 40754-F and CONACyT SEP-2004-C01-47211, as well as by DGAPA-UNAM grant IN104503-3.

References

- [1] J. M. Maldacena, “The large N limit of superconformal field theories and supergravity,” *Adv. Theor. Math. Phys.* **2**, 231 (1998) [*Int. J. Theor. Phys.* **38**, 1113 (1999)] [arXiv:hep-th/9711200].
- [2] S. S. Gubser, I. R. Klebanov and A. M. Polyakov, “Gauge theory correlators from non-critical string theory,” *Phys. Lett. B* **428**, 105 (1998) [arXiv:hep-th/9802109];
E. Witten, “Anti-de Sitter space and holography,” *Adv. Theor. Math. Phys.* **2**, 253 (1998) [arXiv:hep-th/9802150].
- [3] O. Aharony, S. S. Gubser, J. M. Maldacena, H. Ooguri and Y. Oz, “Large N field theories, string theory and gravity,” *Phys. Rept.* **323**, 183 (2000) [arXiv:hep-th/9905111].
- [4] K. Adcox *et al.* [PHENIX Collaboration], “Formation of dense partonic matter in relativistic nucleus nucleus collisions at RHIC: Experimental evaluation by the PHENIX collaboration,” *Nucl. Phys. A* **757**, 184 (2005) [arXiv:nucl-ex/0410003];
I. Arsene *et al.* [BRAHMS Collaboration], “Quark gluon plasma and color glass condensate at RHIC? The perspective from the BRAHMS experiment,” *Nucl. Phys. A* **757** (2005) 1 [arXiv:nucl-ex/0410020];
B. B. Back *et al.*, “The PHOBOS perspective on discoveries at RHIC,” *Nucl. Phys. A* **757** (2005) 28 [arXiv:nucl-ex/0410022];
J. Adams *et al.* [STAR Collaboration], “Experimental and theoretical challenges in the search for the quark gluon plasma: The STAR collaboration's critical assessment of the evidence from RHIC collisions,” *Nucl. Phys. A* **757**, 102 (2005) [arXiv:nucl-ex/0501009].
- [5] F. Carminati *et al.* [ALICE Collaboration], “ALICE: Physics performance report, volume I,” *J. Phys. G* **30** (2004) 1517;
A. Morsch [ALICE Collaboration], “Jet quenching studies with the ALICE detector,” *Czech. J. Phys.* **55** (2005) B333.

- [6] C. P. Herzog, A. Karch, P. Kovtun, C. Kozcaz and L. G. Yaffe, “Energy loss of a heavy quark moving through $N = 4$ supersymmetric Yang-Mills plasma,” arXiv:hep-th/0605158.
- [7] S. S. Gubser, “Drag force in AdS/CFT,” arXiv:hep-th/0605182.
- [8] J. Casalderrey-Solana and D. Teaney, “Heavy quark diffusion in strongly coupled $N = 4$ Yang Mills,” arXiv:hep-ph/0605199.
- [9] C. P. Herzog, “Energy Loss of Heavy Quarks from Asymptotically AdS Geometries,” arXiv:hep-th/0605191.
- [10] E. Cáceres and A. Güijosa, “Drag Force in a Charged $N = 4$ SYM Plasma,” arXiv:hep-th/0605235.
- [11] E. Cáceres and A. Güijosa, “On drag forces and jet quenching in strongly coupled plasmas,” arXiv:hep-th/0606134.
- [12] S. J. Sin and I. Zahed, “Ampere’s law and energy loss in AdS/CFT duality,” arXiv:hep-ph/0606049.
- [13] J. J. Friess, S. S. Gubser and G. Michalogiorgakis, “Dissipation from a heavy quark moving through $N = 4$ super-Yang-Mills plasma,” arXiv:hep-th/0605292.
- [14] Y. h. Gao, W. s. Xu and D. f. Zeng, “Wake of color fields in charged $N = 4$ SYM plasmas,” arXiv:hep-th/0606266.
- [15] J. J. Friess, S. S. Gubser, G. Michalogiorgakis and S. S. Pufu, “The stress tensor of a quark moving through $N=4$ thermal plasma,” arXiv:hep-th/0607022.
- [16] U. H. Danielsson, E. Keski-Vakkuri and M. Kruczenski, “Vacua, propagators, and holographic probes in AdS/CFT,” JHEP **9901**, 002 (1999) [arXiv:hep-th/9812007].
- [17] C. G. Callan and A. Güijosa, “Undulating strings and gauge theory waves,” Nucl. Phys. B **565**, 157 (2000) [arXiv:hep-th/9906153].
- [18] R. Baier, D. Schiff and B. G. Zakharov, “Energy loss in perturbative QCD,” Ann. Rev. Nucl. Part. Sci. **50** (2000) 37 [arXiv:hep-ph/0002198];
R. Baier, “Jet quenching,” Nucl. Phys. A **715**, 209 (2003) [arXiv:hep-ph/0209038].
- [19] A. Kovner and U. A. Wiedemann, “Gluon radiation and parton energy loss,” arXiv:hep-ph/0304151.
- [20] H. Liu, K. Rajagopal and U. A. Wiedemann, “Calculating the jet quenching parameter from AdS/CFT,” arXiv:hep-ph/0605178.

- [21] J. Gomis and F. Passerini, “Holographic Wilson loops,” arXiv:hep-th/0604007.
- [22] J. M. Maldacena, “Wilson loops in large N field theories,” Phys. Rev. Lett. **80** (1998) 4859 [arXiv:hep-th/9803002];
S. J. Rey and J. T. Yee, “Macroscopic strings as heavy quarks in large N gauge theory and anti-de Sitter supergravity,” Eur. Phys. J. C **22** (2001) 379 [arXiv:hep-th/9803001].
- [23] A. Buchel, “On jet quenching parameters in strongly coupled non-conformal gauge theories,” arXiv:hep-th/0605178.
- [24] J. F. Vazquez-Poritz, “Enhancing the jet quenching parameter from marginal deformations,” arXiv:hep-th/0605296.
- [25] S. J. Sin and I. Zahed, “Holography of radiation and jet quenching,” Phys. Lett. B **608** (2005) 265 [arXiv:hep-th/0407215]
- [26] E. Shuryak, S. J. Sin and I. Zahed, “A gravity dual of RHIC collisions,” arXiv:hep-th/0511199.
- [27] F. L. Lin and T. Matsuo, “Jet quenching parameter in medium with chemical potential from AdS/CFT,” arXiv:hep-th/0606136.
- [28] S. D. Avramis and K. Sfetsos, “Supergravity and the jet quenching parameter in the presence of R-charge densities,” arXiv:hep-th/0606190.
- [29] N. Armesto, J. D. Edelstein and J. Mas, “Jet quenching at finite ’t Hooft coupling and chemical potential from AdS/CFT,” arXiv:hep-ph/0606245.
- [30] S. J. Rey, S. Theisen and J. T. Yee, “Wilson-Polyakov loop at finite temperature in large N gauge theory and anti-de Sitter supergravity,” Nucl. Phys. B **527** (1998) 171 [arXiv:hep-th/9803135].
- [31] A. Brandhuber, N. Itzhaki, J. Sonnenschein and S. Yankielowicz, “Wilson loops in the large N limit at finite temperature,” Phys. Lett. B **434**, 36 (1998) [arXiv:hep-th/9803137].
- [32] K. Peeters, J. Sonnenschein and M. Zamaklar, “Holographic melting and related properties of mesons in a quark gluon plasma,” arXiv:hep-th/0606195.
- [33] H. Liu, K. Rajagopal and U. A. Wiedemann, “An AdS/CFT Calculation of Screening in a Hot Wind,” arXiv:hep-ph/0607062.
- [34] I. R. Klebanov, J. M. Maldacena and C. B. Thorn, “Dynamics of flux tubes in large N gauge theories,” JHEP **0604** (2006) 024 [arXiv:hep-th/0602255].
- [35] E. Witten, “Baryons and branes in anti de Sitter space,” JHEP **9807**, 006 (1998) [arXiv:hep-th/9805112].

- [36] Y. Imamura, “Supersymmetries and BPS configurations on Anti-de Sitter space,” Nucl. Phys. B **537** (1999) 184 [arXiv:hep-th/9807179].
- [37] C. G. Callan, A. Güijosa and K. G. Savvidy, “Baryons and string creation from the fivebrane worldvolume action,” Nucl. Phys. B **547** (1999) 127 [arXiv:hep-th/9810092];
C. G. Callan, A. Güijosa, K. G. Savvidy and O. Tafjord, “Baryons and flux tubes in confining gauge theories from brane actions,” Nucl. Phys. B **555**, 183 (1999) [arXiv:hep-th/9902197].
- [38] K. Rajagopal, private communication.
- [39] U. A. Wiedemann, private communication.
- [40] L. Susskind and E. Witten, “The Holographic Bound In Anti-De Sitter Space,” arXiv:hep-th/9805114;
A. W. Peet and J. Polchinski, “UV/IR relations in AdS dynamics,” Phys. Rev. D **59** (1999) 065011 [arXiv:hep-th/9809022].